

Self-formed straight rivers with equilibrium banks and mobile bed. Part 2. The gravel river

By GARY PARKER

Department of Civil Engineering, University of Alberta,
Edmonton, Canada T6G 2G7

(Received 26 May 1977 and in revised form 3 March 1978)

Rivers are capable of transporting their own bed material without altering their width. However, a naive extension of the threshold theory of canals in coarse alluvium to straight reaches of gravel rivers leads to the stable-channel paradox: transport of bed material is incompatible with a stable width. In this paper singular perturbation techniques are used to obtain a bed stress distribution which allows a mobile bed but immobile banks at bankfull or dominant discharge. This result is used to obtain regime relations for straight rivers with bed and banks composed of coarse gravel.

The analysis, although dependent on a series of approximate assumptions for Reynolds-stress closure and sediment transport, provides reasonable agreement with data.

1. Introduction

Alluvial rivers possess channels that are self-formed by the interaction of water and sediment. They thus present a novel fluid flow problem in which one is asked to determine not only the flow in a given 'container', but also the geometry of the 'container' itself.

The general problem is the prediction of stable, morphologically active river channels, i.e. a channel that can transport most of the available sizes of its own bed material without immediately eroding or narrowing its banks. In part 1 (Parker 1978) the case of the suspendable sand-silt channel was analysed, and stable channels were delineated in terms of a dynamic equilibrium between bank erosion and bank deposition. The present paper analyses the case of channels in which the bed and banks are composed of gravel of sufficient coarseness to preclude its suspension. It is shown that the banks can induce a lateral redistribution of stress such that the bed is mobile, although the banks are in static equilibrium.

2. Natural coarse-gravel rivers

A description of some of the salient features of rivers with a coarse-gravel bed and banks provides a basis for abstraction to a realistic but tractable model. The Athabasca River near Fort Assiniboine, Alberta, illustrated in figure 1 (plate 1), provides an example of a large (mean discharge is 310 m³/s) river in coarse gravel. An analysis of the hydraulic and morphologic characteristics of this reach has been performed by Neill (1973). Both the bed and the banks are composed essentially of very coarse gravel. From bar samples it was found that D_{90} (sediment equivalent diameter such

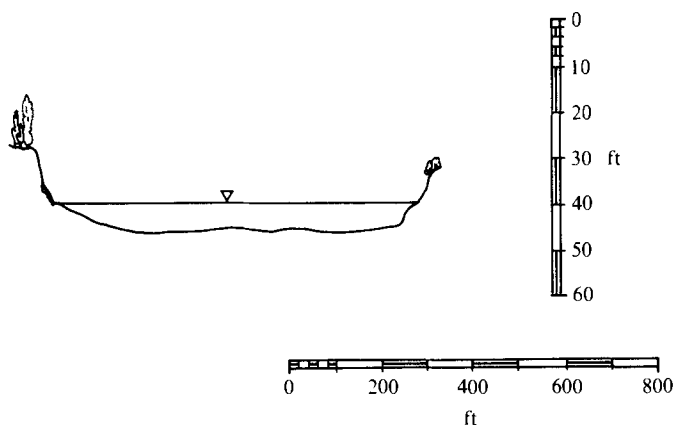


FIGURE 2. Cross-section of a straight reach of the Athabasca River (from Neill 1973).

that 90% of a given sample is smaller) is 75 mm, D_{50} is 45 mm and D_{10} is somewhat less than 4 mm. Although the river lies in a deep postglacial valley, the valley is wide enough so that in many places the river flows through its own alluvium without impinging on the valley walls. In these places the river channel is self-formed. The presence of shifting bars illustrates that at large discharges the river is capable of transporting the majority of sizes of its bed material. However, the rate of transport of bed material appears to be small, and to be almost exclusively as bed load for sizes larger than D_{10} . The river exhibits considerable shifting associated with alignment variation, but many cross-sections have remained stable through a series of floods, and the average characteristics of the reach appear to have been stable in historic time. A typical cross-section in a straight portion is given in figure 2.

A parameter indicative of bed mobility is the Shields stress $\bar{\tau}^*$ based on reach and cross-sectional average properties, which is given by

$$\bar{\tau}^* = \bar{D}S/\mathcal{R}D_{50},$$

where \bar{D} is the average depth, S is the average water surface slope, ρ_s and ρ are, respectively, the sediment and water density and $\mathcal{R} = \rho_s/\rho - 1$ ($= 1.65$ for natural material). Neill (1968) suggests an absolute lower bound for sediment movement in gravel of $\bar{\tau}^* = 0.03$. On the Athabasca River, Neill finds that at a 'dominant' discharge of $2700 \text{ m}^3/\text{s}$ (somewhat below bankfull) $\bar{\tau}^*$ is typically about 0.042 .

Thus, although sediment transport occurs, $\bar{\tau}^*$ does not exceed the critical value for movement by much. This observation, which is important to the present analysis, is found to be true for many (but not all) gravel rivers. Kellerhals (1963; see also Kellerhals 1967) has examined seven reaches of rivers in British Columbia, Canada. Four of the reaches are at the outlet of lakes, where it can be expected that sediment transport vanishes. For the three reaches in which sediment can be expected to be transported at higher discharges - Cariboo River at Quesnel Forks, Quesnel River at Lawless Creek and Chilko River at Henry's Crossing - the value of $\bar{\tau}^*$ based on an arbitrary 'dominant' discharge was found to range no higher than about 0.043 . Although Brush (1961) does not give information concerning bank material, moderate



FIGURE 1. Athabasca River near Whitecourt during spring breakup.
Photo courtesy of the Alberta Research Council.

Shields stresses are observed on most of the larger gravel-bed streams he surveyed in Pennsylvania, U.S.A.; Shaver Creek is typical, with values of $\bar{\tau}^*$ of about 0.054.

While streams with gravel beds which sustain much higher values of $\bar{\tau}^*$ can also be found (Hollingshead 1971), the case of near-critical Shields stress concurrent with sediment transport appears to represent a limiting case applying to straight equilibrium reaches of rivers with beds and banks of loose gravel of similar size.

Thus the case of a straight channel of symmetrical cross-section with bed and banks composed of loose similar gravel is analysed herein. Such a channel must be able to withstand bankfull or dominant discharges without bank erosion, even though sediment is in transport on the bed.

Self-formed gravel channels can be modelled in the laboratory with the use of coarse sand, as has been done by Wolman & Brush (1961); again it is found that straight channels with low but non-vanishing bed load and values of $\bar{\tau}^*$ of about 0.040 are formed. The analysis applies to these channels as well in so far as the flow is hydraulically rough.

3. Threshold theory of stable canals

The only successful rational derivation of channel geometry available at present is that due to Glover & Florey (1951), in which a canal cross-section of minimum area such that sediment is on the threshold of motion everywhere is determined. The analysis is not applicable to most natural rivers in that it predicts vanishing sediment transport. It will nevertheless prove useful to review a modified version due to Lane, Lin & Liu (1959; as reported in Li, Simons & Stevens 1976).

A symmetrical cross-section of width B and centre depth D_c in uniformly distributed coarse alluvium is considered. The lateral co-ordinate y is measured from the centre of the channel. The time-averaged bed stress distribution, assumed to be critical everywhere, is $\tau = \tau_c(y)$ (figure 3), and depth is $D(y)$.

The use of a time-averaged critical stress implies that, under the associated mean conditions, sediment does not move at some larger 'effective' stress $\alpha\tau_c(y)$ the probability of which is vanishingly small. The mean lift per unit area is $\beta\tau_c$, where $\beta \simeq 0.85$, and the 'effective' lift per unit area is taken to be $\alpha\beta\tau_c$.

The appropriate form for the momentum balance for equilibrium flow in a channel with depth D_c and infinite width is

$$\tau = \rho g D_c S,$$

where g is the acceleration due to gravity. A number of naive formulations for momentum balance in the channel illustrated in figure 3 exist. Perhaps the most complete is the area formula of Lundgren & Jonsson (1964), in which the resistive force $\tau dP \Delta x$ on a portion of bed of longitudinal extent Δx and lateral arc length dP is balanced by the downstream component of the weight of the water with volume $dA \Delta x$, where dA is the cross-sectional area above dP bounded by normals to the bed (figure 4). It is thus found that

$$\tau = \rho g \frac{dA}{dP} S = \left(D \left/ \cos \theta + \frac{1}{2} \cos \theta D^2 \frac{d^2 D}{dy^2} \right. \right) \rho g S, \quad (1)$$

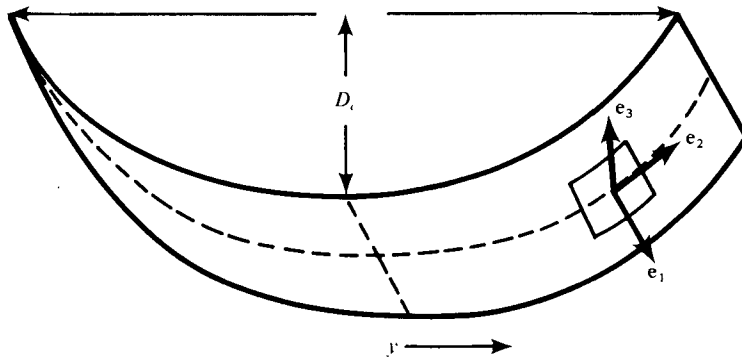


FIGURE 3. Definition diagram for derivation of threshold canal geometry.

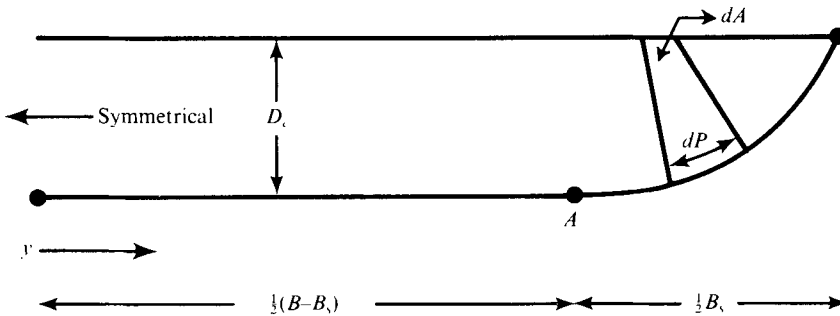


FIGURE 4. Definition diagram outlining assumed channel geometry of straight reaches of coarse-gravel rivers.

where θ is the local lateral angle of inclination. This formula can be simplified considerably for appropriately wide channels. If $\tilde{\epsilon} = (2D_c/B)^2$, then for small $\tilde{\epsilon}$ the above formula can be expanded as

$$\tau/\rho g S D = 1 + O(\tilde{\epsilon}).$$

Since $\cos \theta = 1 + O(\tilde{\epsilon})$, it is found that the momentum balance may be written, to lowest order, as

$$\tau = \rho g D S \cos \theta. \tag{2}$$

The cosine term is inserted since it will allow closed-form integration to be performed shortly.

Let P_1 be the bed porosity and μ be the submerged static coefficient of Coulomb friction. Furthermore let $\{e_1, e_2, e_3\}$ be a set of orthogonal unit vectors such that e_1 is downstream and tangential to the bed, e_2 is outward and tangential to the bed, and e_3 is upward and normal to the bed (figure 3). The force balance on an arbitrary area of the bed surface one grain thick is considered. Particles are pulled downstream by fluid stress and inward under the influence of gravity (the analysis neglects secondary currents). The effective stress vector T_{ET} tangential to the bed is

$$T_{ET} = \alpha \tau_c e_1 - \rho \mathcal{R} g (1 - P_1) D_{50} \sin \theta e_2. \tag{3}$$

The effective stress T_{EN} normal to the bed is

$$T_{EN} = -[\rho \mathcal{R} g (1 - P_1) D_{50} \cos \theta - \alpha \beta \tau_c] e_3. \tag{4}$$

The condition for incipient motion is that the Coulomb friction force should just balance the tangential erosive forces:

$$|\mathbf{T}_{ET}| = \mu |\mathbf{T}_{EN}|. \quad (5)$$

At the centre, where $y = 0$, $\theta = 0$; if $\tau_{c0} \equiv \tau_c(0)$, then from (5)

$$\tau_{c0} = \frac{\mu(1 - P_1)}{\alpha(1 + \mu\beta)} \rho \mathcal{R} g D_s,$$

or in terms of critical Shields stress $\tau_{c0}^* = \tau_{c0} / \rho \mathcal{R} g D_s$,

$$\tau_{c0}^* = \mu(1 - P_1) / \alpha(1 + \mu\beta). \quad (6)$$

For coarse sediment μ is assumed to take the value 0.84, corresponding to an angle of repose of 40° , and an appropriate value for P_1 is 0.35. The value of α corresponding to $\tau_{c0}^* = 0.03$ is seen to be 10.6.

Rearranging (5) according to (2), (6) and the relation $\tan \theta = -dD/dy$ gives

$$\left(\frac{D}{D_c}\right)^2 + \left(\frac{1 + \mu\beta}{\mu}\right)^2 \left(\frac{dD}{dy}\right)^2 = \mu^2 \left(\frac{1 + \mu\beta}{\mu} - \beta \frac{D}{D_c}\right)^2. \quad (7)$$

Two boundary conditions must be satisfied:

$$D(0) = D_c, \quad D(\frac{1}{2}B) = 0. \quad (8)$$

Equation (7) is of first order, so the two boundary conditions overspecify the problem and imply a relation among D_c , B , β and μ . The solution to (7) and (8) is found by direct integration:

$$\frac{D}{D_c} = \frac{1}{1-r} \left[\cos \left\{ \mu \left(\frac{1-r}{1+r} \right)^{\frac{1}{2}} \frac{y}{D_c} \right\} - r \right], \quad (9a)$$

$$\tilde{\epsilon}^{\frac{1}{2}} = \frac{2D_c}{B} = \mu \left(\frac{1-r}{1+r} \right)^{\frac{1}{2}} \frac{1}{\cos^{-1} r}, \quad (9b)$$

where $r = \beta\mu$. For the values previously cited for β and μ , $\tilde{\epsilon} = 0.20$, a value small enough to justify the approximation embodied in (2).

The critical-stress theory, in conjunction with an appropriate resistance relation, allows complete delineation of the canal geometry of minimum cross-sectional area at threshold conditions. If D_{50} and any two of the parameters D_c , B , Q and S are specified, the other two parameters and the channel geometry can be calculated.

An important point is that for threshold channels the aspect ratio $\mathcal{A} = B/D_c$ is given by

$$\mathcal{A} = 4.5. \quad (10)$$

4. The stable-channel paradox

The threshold theory of canals does not apply to most rivers in that no sediment transport occurs. The case where sediment is transported is now considered. The bed stress is calculated from the area formula (1).

Some volumetric sediment load Q_s is imposed on the river. In order for this load to be transported the stress $\tau(y)$ must be greater than $\tau_c(y)$ for a finite range of values of

y near the centre. Any grain thus put in motion will be subject not only to a downstream force, but also to an inward force as well, as seen from (3). Thus grains are transported down the bank to the centre of the channel, and bank erosion is accomplished. As long as a load is imposed bank erosion must continue and the channel must widen indefinitely. Conversely, if the channel is to be stable then the load must vanish. This was first delineated by Hirano (1973).

In short, sediment transport is incompatible with a stable channel. This is termed the 'stable-channel paradox' since it indicates that stable rivers in coarse alluvium cannot exist.

The paradox cannot be resolved by placing a stretch of constant depth D_c in between the two 'bank regions' as in figure 4. Since the 'bank regions' join the centre 'bed region' smoothly, (1) indicates that if the stress is above critical on the bed region then it must be above critical somewhere on the bank region, and bank erosion will again occur.

A simple order-of-magnitude analysis, similar to that in part 1, can be used to show that lateral stresses induced by straight-channel secondary currents are typically much smaller than the lateral erosive stress due to gravity in (3). It thus appears unlikely that secondary currents can be invoked directly to resolve the paradox. (They may, however, play an indirect role, as discussed in § 5.)

Li *et al.* (1976) have argued that very small cobble streams are in fact threshold channels of the type described by (9). They circumvent the stable-channel paradox by arguing that any load consists of particles that are considerably (two to three times) smaller than the dominant size of the channel itself. Such a load could be called 'throughput load' since it is not related to the channel geometry. Two consequences of this assumption illustrate that its applicability to gravel rivers is limited.

The first is that such a channel would be incapable of shifting; also, any bedforms must be composed of throughput load. Gravel rivers, however, usually show a proclivity for shifting (Kellerhals, Neill & Bray 1972). Data from, for example, the Athabasca River indicate that material coarser than the median bed material size is common on bars, and could only have been transported to such locations.

The second consequence is that the aspect ratio \mathcal{A} should have a value of about 4.5 at bankfull or dominant discharge. This value is unrealistically low for most cases of interest. For the Athabasca River near Fort Assiniboine, for example, the value of \mathcal{A} on straight reaches at dominant discharge is in the range 40–65.

The available evidence indicates that most gravel rivers are capable of maintaining grossly stable widths while transporting most of the available sediment sizes. This applies locally to straight reaches and globally to average cross-sections of long reaches, the averaging being introduced to eliminate the effect of changing alignment. The very existence of such rivers appears to be paradoxical.

5. A resolution based on turbulent momentum transfer

'Paradoxes' such as the stable-channel paradox are often resolved in terms of singular perturbation analysis (e.g. D'Alembert's paradox). Such a resolution is proposed herein.

The geometry of figure 4 is considered. The channel has a total width B , a flat bed region of width $B - B_s$ where the depth is D_c , and on either side of this a bank region of width $\frac{1}{2}B_s$ where the depth varies smoothly from D_c at the junction point A to zero at the bank. The y co-ordinate is measured from the channel centre. The arc length P and area $A(P)$ are the quantities defined previously.

The downstream velocity, and thus the momentum, is greater near the channel centre than near the banks. Turbulence can be expected to produce a net lateral flux of longitudinal momentum from regions of high momentum to regions of low momentum, i.e. from the centre region to the bank region. This results in a deficit of bed stress compared with that predicted by (1) near the centre and a surfeit near the banks. It is this lateral transfer of momentum that is responsible for the maintenance of wall stress in rectangular flumes (Cruff 1965).

Another, usually weaker, mechanism that can also induce lateral transfer of longitudinal momentum is embodied in straight-channel secondary currents, which typically consist of cells so oriented as to move longitudinal momentum into 'corners' (the water margin in this case).

In order to illustrate the process, the equation of longitudinal momentum balance, integrated along a normal to the bed, is considered. Let z be normal distance from the bed, $D_N = D/\cos\theta$ be normal depth, U and u' be, respectively, the mean and fluctuating downstream flow velocities and V and v' be the mean and fluctuating cross-stream velocities in the direction of \mathbf{e}_2 (figure 4). It is found that

$$\tau = \rho g S \frac{dA}{dP} - \frac{d}{dP} \int_0^{D_N} (\rho \overline{u'v'} + \rho U V) dz. \quad (11)$$

Note, then, that the area method (1) must be corrected for the lateral turbulent transport rate of downstream momentum

$$M_T(P) = \int_0^{D_N} \rho \overline{u'v'} dz$$

and the lateral transport rate of downstream momentum due to secondary currents

$$M_S(P) = \int_0^{D_N} \rho U V dz.$$

Lundgren & Jonsson (1964) suggest that $M_S(P)$ is the weaker of the two and that it may be neglected in a first-order analysis. This procedure is adopted herein. It is, however, noted that this point deserves further investigation.

The lateral transport of longitudinal momentum M_T is assumed to be directed towards the banks on the physical grounds outlined above, and must vanish in the centre (owing to symmetry) and at the banks (where the bed meets the water surface). It may be surmised to have the form given in figure 5 and when inserted into (11) gives the stress redistribution discussed above, which is illustrated in the same figure in terms of the stress depth $\delta(y) = \tau(y)/\rho g S$.

Such a stress distribution has the prerequisites for resolving the stable-channel paradox. The stress is observed to be a smooth, monotonically decreasing function of y . By appropriately adjusting the channel depth, the stress could be at or below critical on the entire bank region, but would then increase to a value above critical on at least

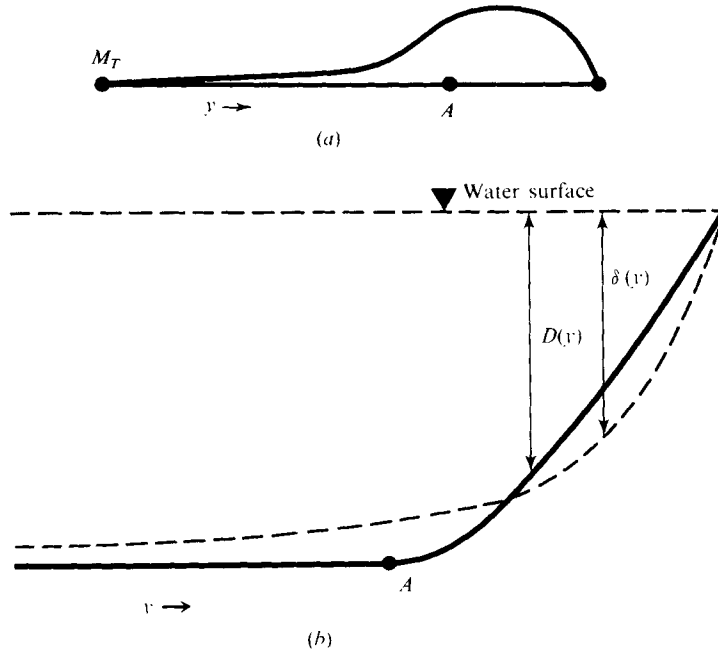


FIGURE 5. (a) Lateral flux of downstream momentum M_T as a function of lateral distance from channel centre. (b) Resulting stress redistribution in terms of stress depth $\delta(y)$.

part of the bed region. Thus the banks would remain stable, even though sediment transport would occur on the bed.

In order to make the problem amenable to quantitative analysis, it is first necessary to close (11). Lundgren & Jonsson (1964) use two simple assumptions to accomplish this. The first, due to Leighly (1932), is that lines of vanishing cross-sectional shear stress and momentum flux are orthogonal to the isovels. The second states that the logarithmic rough-wall law appropriate for flat beds and pipes holds throughout the flow along normals to the bed. (This assumption was first introduced in a primitive form by Keulegan 1938.) Thus if $u_* = (\tau/\rho)^{1/2}$ and k is bed roughness,

$$U(z)/u_* = 2.5 \ln(30z/k). \tag{12}$$

Both assumptions are known to be incorrect for many flows, and strictly apply only to the case of small lateral bed curvature. Some error may also be expected in applying the logarithmic law in the core region of the flow.

The closure obtained for M_T by Lundgren & Jonsson under these assumptions and the additional proviso of small lateral bed curvature is

$$M_T = -D_N^2 \psi \left(j, \frac{D_N}{k} \right) \frac{d\tau}{dP},$$

where

$$\psi \left(j, \frac{D_N}{k} \right) = \left[\frac{4+j}{24(2-j)} \ln \left(30 \frac{D_N}{k} \right) - \frac{5}{36(2-j)} \right] \left[1 + \frac{1}{2 \ln(30D_N/k) - \frac{17}{3}} \right],$$

and $j = -D_N D_{yy} / [1 + (D_y)^2]^{3/2}$ is the dimensionless channel curvature. Equation (11), expressed in terms of the stress depth $\delta = \tau/\rho g S$, can then be written as

$$\delta = D_N(1 - \frac{1}{2}j) + \frac{d}{dP} D_N^2 \psi \frac{d\delta}{dP}. \tag{13}$$

Equation (13) applies to the case of small lateral bed curvature $j \sim \epsilon$, where $\epsilon = (2D_c/B_s)^2$. This suggests that the term of highest order in (13) is small, leading to an asymptotic expansion for δ in ϵ in which the lowest-order term is given by the area method:

$$\delta \simeq D_N(1 - \frac{1}{2}j).$$

Such a scheme, which was used successfully by Lundgren & Jonsson in channels of the type of figure 3, fails for the geometry of figure 4 because it predicts a discontinuity in δ at the junction point A . It thus cannot be used to resolve the stable-channel paradox. This non-uniform behaviour is due to the neglect of the highest-order derivative in (13) in the lowest-order approximation, and must be resolved with the use of singular perturbation techniques. The resulting solution can then be applied to the prediction of gravel-river geometry.

6. Solution of Lundgren & Jonsson's equation

In the bed region of the channel in figure 4, the depth takes the constant value D_c and (13) reduces to

$$\delta = D_c + \psi(0, R_k) D_c^2 d^2\delta/dy^2, \tag{14}$$

where $R_k = D_c/k$ is the relative roughness. Since the stress profile is to be symmetric in y , the boundary condition $[d\delta/dy]_{y=0}$ must hold. A solution to (14) subject to this boundary condition is

$$\delta/D_c = 1 + \bar{C} \cosh(\alpha y/D_c), \tag{15}$$

where $\alpha = \psi(0, R_k)^{-\frac{1}{2}}$. The constant \bar{C} must be determined by matching this bed solution to a bank solution under the conditions that δ and $d\delta/dy$ be continuous at the junction point.

It is necessary to specify the depth profile before bank solutions can be obtained. On the right bank region of figure 4, as the bank region is traversed from junction to bank y varies from $\frac{1}{2}(B - B_s)$ to $\frac{1}{2}B$ and D must vary smoothly from D_c to zero. Thus at the junction point the conditions

$$D|_{y=\frac{1}{2}(B-B_s)} = D_c, \quad [dD/dy]_{y=\frac{1}{2}(B-B_s)} = 0 \tag{16a, b}$$

must be satisfied and at the water's edge the condition

$$D|_{y=\frac{1}{2}B} = 0 \tag{16c}$$

must hold. Furthermore $D(y)$ must be such that no bank erosion occurs.

Apart from these general conditions, the depth profile is left arbitrary at this point. In non-dimensional form, the depth profile is expressed as

$$s = f(\eta),$$

where $s = D/D_c$, $\eta = y/\frac{1}{2}B_s - (1 - \epsilon_1)/\epsilon_1$ and $\epsilon_1 = B_s/B$. The parameter η varies from 0 to 1 and s varies from 1 to 0 as the bank region is traversed. The conditions (16) give

$$f(0) = 1, \quad f'(0) = 0, \quad f(1) = 0, \tag{17}$$

where the prime denotes differentiation with respect to η .

Equation (13) is now solved on the bank region in terms of an asymptotic expansion in $\epsilon = (2D_c/B_s)^2$, a parameter estimating lateral bank curvature that is assumed to be small. In terms of the dimensionless stress depth $\sigma = \delta/D_c$, (13) takes the form

$$\sigma = s\{1 + \frac{1}{2}\epsilon[(s_\eta)^2 + s_{\eta\eta}s]\} + c d[\psi(0, R_k s) s^2 \sigma_\eta]/d\eta + O(\epsilon^2). \tag{18}$$

Equation (18) is of second order, and its general solution contains two free constants. Three boundary conditions apply. For smooth matching with the bed solution, σ and σ_η must equal the corresponding values of the bed solution at the junction. Furthermore σ must vanish at $\eta = 1$. These conditions allow evaluation of the two constants in the bank solution and the free constant \bar{C} in the bed solution.

It is seen that for small ϵ the equation approximates to $\sigma \simeq s$. More formally, an asymptotic expansion of the form

$$\sigma = \bar{\sigma}_0 + \epsilon \bar{\sigma}_1 + \dots \quad (19)$$

is assumed; substituting into (18), it is found that

$$\bar{\sigma}_0 = s, \quad \bar{\sigma}_1 = \frac{1}{2}[s(s_\eta)^2 + s^2 s_{\eta\eta}] + d[\psi(0, R_k s) s^2 s_\eta] / d\eta. \quad (20a, b)$$

An attempt to match this approximate solution with the bed solution fails. The only free constant is \bar{C} so the two conditions of matched σ and σ_η cannot be satisfied simultaneously, and non-uniform behaviour results at the junction.

The problem is due to the fact that the approximate solution (20) is obtained at the expense of dropping all terms containing derivatives of the dependent variable σ in (18). As the equation is of second order, two free constants which would allow matching are lost, and (20) cannot be valid everywhere.

In particular, there must exist a thin region near the junction $\eta = 0$ where the stress gradient σ_η is so steep that terms containing $\sigma_{\eta\eta}$ are not negligible. Such a region is termed a boundary layer (but resembles Prandtl's boundary layer only in the mathematical sense, i.e. it is associated with non-uniform behaviour due to the neglect of the highest-order derivatives).

The expansion which leads to non-uniform behaviour is conventionally termed the outer expansion; in this case (19) is the outer bank expansion and η is the outer variable.

It is necessary to find an inner expansion valid in a thin layer located near $\eta = 0$. From dimensional considerations, the boundary layer is found to have thickness $\epsilon^{\frac{1}{2}}$, and an appropriate inner variable is seen to be $p = \eta / \epsilon^{\frac{1}{2}}$. The inner expansion is of the form

$$\sigma = \sigma_0 + \epsilon \sigma_1 + \dots \quad (21)$$

Note that

$$s = f(\epsilon^{\frac{1}{2}}p) = 1 + \frac{1}{2}\epsilon f_{\eta\eta}(0)p^2 + O(\epsilon^2).$$

The equation for the stress depth becomes

$$\sigma = 1 - \epsilon\gamma(1 + p^2) + \{A - \epsilon\gamma[2B + (2A + C)p^2]\} \frac{d^2\sigma}{dp^2} - 2\epsilon\gamma(2A + C) \frac{d\sigma}{dp} + O(\epsilon^2), \quad (22)$$

where $\gamma = -\frac{1}{2}f_{\eta\eta}(0)$ (γ is positive for the physically applicable case of an upward-curving bank region) and

$$A = \psi(0, R_k) = \frac{1}{\alpha^2}, \quad B = -\frac{\partial\psi}{\partial a}(0, R_k), \quad C = R_k \frac{\partial\psi}{\partial b}(0, R_k),$$

$$a = -ss_{pp}[1 + (s_p)^2]^{-\frac{3}{2}}, \quad b = R_k s.$$

From (21) and (22) it is found that

$$\sigma_0 = 1 + Ad^2\sigma_0/dp^2, \quad (23a)$$

$$\sigma_1 = -\gamma \left\{ 1 + 2B \frac{d^2\sigma_0}{dp^2} + 2(2A + C) \frac{d\sigma_0}{dp} + \left[1 + (2A + C) \frac{d^2\sigma_0}{dp^2} \right] p^2 \right\} + A \frac{d^2\sigma_1}{dp^2}. \quad (23b)$$

The solution to (23a) is

$$\sigma_0 = C_1 e^{\alpha p} + C_2 e^{-\alpha p} + 1.$$

The inner bank solution must match with both the bed solution ('left matching') and the outer bank solution ('right matching'). In order to facilitate left matching, the constant \bar{C} in (15) is expanded asymptotically in ϵ :

$$\bar{C} = \bar{C}_0 + \epsilon \bar{C}_1 + \dots$$

Right matching (the outer expansion of the inner expansion must equal the inner expansion of the outer expansion) imposed to lowest order requires that $C_1 = 0$. Left matching (σ and σ_p must be continuous) imposed to lowest order requires that $\bar{C} = C_2 = 0$, in which case

$$\sigma_0 = 1. \tag{24}$$

Progressing to the next higher order, the general solution to (23b) is

$$\sigma_1 = \check{C}_1 e^{\alpha p} + \check{C}_2 e^{-\alpha p} - \gamma(1 + 2A + p^2).$$

Again, right matching with (20b) is satisfied if $\check{C}_1 = 0$. The results of left matching are

$$\check{C}_2 = \frac{\gamma(1 + 2A)}{1 + \coth \theta}, \quad \bar{C}_1 = \frac{-\gamma(1 + 2A)}{\sinh \theta(1 + \coth \theta)},$$

where

$$\theta = \frac{1}{A^{\frac{1}{2}}}(1 - \epsilon_1) \frac{1}{\epsilon_1 e^{\frac{1}{2}}}.$$

Thus the solution of (13) is complete to first order in ϵ on all regions of the bed.

It should be noted that an extension of the perturbation scheme to higher orders is unwarranted in that such terms were neglected in the derivation of (13).

The bed stress on the bed region is given to first order by

$$\frac{\delta}{D_c} = 1 - \epsilon \frac{\gamma(1 + 2A)}{\sinh \theta + \cosh \theta} \cosh \left(\frac{1}{A^{\frac{1}{2}}} \frac{y}{D_c} \right). \tag{25}$$

Since θ , γ and A are positive for physically admissible cases, this equation indicates a stress deficiency on the bed region scaled by ϵ , which becomes progressively more severe as the bank region is approached. This is exactly the condition that has been postulated to allow the coexistence of bed sediment transport and stable banks in non-cohesive gravel channels.

7. The bank region of a self-formed straight gravel river

The lateral depth profile of the bank region of a straight gravel river at bankfull or dominant discharge must be one that specifies critical conditions everywhere, if the river is to be self-formed. This provides a means of evaluating the bank profile, heretofore left arbitrary except for certain general conditions.

If stress is critical everywhere on the bank region, then σ must satisfy the dimensionless form of (5), reduced with (6):

$$\left(\frac{\sigma}{\sigma_c} \right)^2 + \frac{1+r}{\mu} \sin^2 \theta = \left[r \cos \theta - \beta \left(\frac{\sigma}{\sigma_c} \right) \right]^2, \tag{26}$$

where σ_c is the dimensionless critical stress at the junction point. But on all of the bank region except the boundary layer near the junction point, it is seen from (20) that

$$\sigma = s + O(\epsilon). \quad (27)$$

Note that $\cos \theta = 1 + O(\epsilon)$, so that to lowest order (27) can be written as $\sigma = s \cos \theta$. Inserting this into (26) and solving for s subject to the (overspecified) boundary conditions $s(0) = 1$ and $s(1) = 0$, the solution is found to be

$$s = \frac{1}{1-r} [\cos(\eta \cos^{-1} r) - r], \quad (28)$$

$$\epsilon = \left(\frac{\mu}{\cos^{-1} r} \right)^2 \left(\frac{1-r}{1+r} \right). \quad (29)$$

Thus the threshold solution cited in § 3 is recovered as the shape for the bank region.

The value of ϵ applicable to self-formed gravel rivers is seen to be 0.20. While this value is not exceedingly small it is nevertheless small enough to render appropriate the expansion techniques used herein.

The constant γ can be evaluated from (28):

$$\gamma = (\cos^{-1} r)^2 / 2(1-r) = 1.05.$$

8. Towards rational regime relations for straight reaches

The preceding analysis, combined with a resistance relation and a sediment transport relation, allows the derivation of regime relations for gravel rivers at bankfull or estimated 'dominant' discharges; the latter is appropriate for streams entrenched well below their flood plains.

Three major factors contribute to the resistance of gravel rivers: grain, dune and alignment (bar) resistance. The last can be neglected in a straight reach. Dunes in gravel tend to be poorly developed and often contribute little to the total resistance. It is reasonable to approximate the resistance to be entirely grain resistance with a roughness height $k = D_{90}$. Integration of (12) over an infinitely wide channel with constant depth D then gives

$$\bar{U}/u_* = 2.5 \ln(11D/D_{90}), \quad (30)$$

where \bar{U} is the vertically averaged velocity.

This resistance relation was tested with the experimental and field data corresponding to moving gravel among the more than 6000 data sets contained in the compendium of Peterson & Howells (1973). Only data explicitly including the temperature and particle distribution gradation were selected. Aspect ratios $\mathcal{A} < 5$ were not included, so that a division into wall and bed stress would not be required. D_{90} was calculated from the given D_{50} , the gradation and the assumption of a Gaussian distribution. The requirement $R_p = (\mathcal{R}gD_{50})^{1/2} D_{50}/\nu > 500$ assured that all data were in the gravel range and the requirement $u_* D_{90}/\nu > 70$ assured that the flow was hydraulically rough. The 278 data sets satisfying these conditions are plotted on figure 6 with (30); nearly all points are experimental rather than field. The closed circles correspond to natural bed material ($\mathcal{R} = 1.65$) and the open circles to artificial bed material ($\mathcal{R} \neq 1.65$). While the considerable scatter associated with mobile beds is evident, the fit is reasonable.

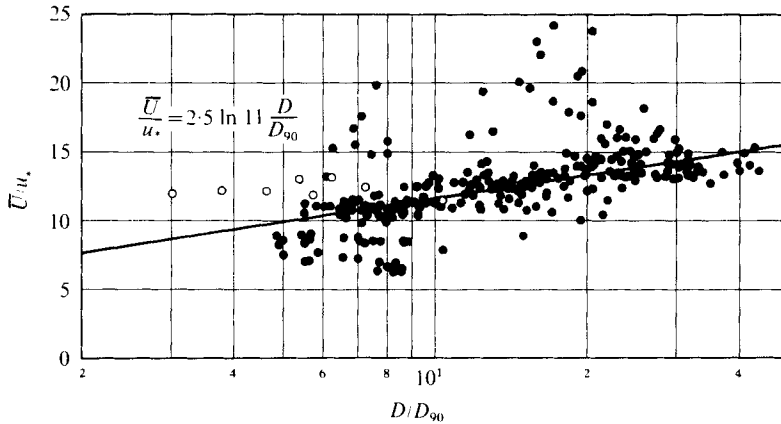


FIGURE 6. Resistance relation for gravel beds.

The same data were used to determine a bed load relation. The Einstein sediment discharge $q^* = q/[(\mathcal{R}gD_{50})^{1/2} D_{50}]$, where q = volumetric bed load discharge per unit width, is plotted against the Shields stress $\tau^* = \tau/\rho\mathcal{R}gD_{50}$ in figure 7. The data, which show a very steep relationship between q^* and τ^* , were fitted by eye to the relation

$$q^* = 11.2(\tau^* - 0.03)^{4.5}\tau^{*-3}. \tag{31}$$

This equation, while representing a reasonable fit, is included primarily for illustrative purposes and could be replaced by a more reliable relation based on field data.

The first regime relation can be obtained from the fact that the stress in (25) must be equal to the critical value at the junction point under bankfull or dominant conditions:

$$\frac{D_c S}{\mathcal{R}D_{50}} \left(1 - \epsilon \frac{\gamma(1+2A)}{1 + \tanh \theta} \right) = \tau_c^*. \tag{32}$$

This relation thus predicts depths on the bed region that are $O(\epsilon)$, or about 20%, above critical. Defining the parameters $R = D_c/D_{50}$ and $e = D_{50}/D_{90}$, (32) can be accurately approximated by the power-law form

$$R = 0.0553S^{-1.01} \tag{33}$$

for $\mathcal{R} = 1.65$ (natural material) and for the ranges $8 < R < 140$, $\mathcal{A} > 15$ and typical values of e (0.4–0.6). Equation (33) is the first regime relation. It is remarkable that this relation and relation (36) of part 1 should be similar, both relating R to S independently of the aspect ratio, water discharge and sediment discharge, even though the mechanisms involved are entirely different.

The second and third regime relations can be obtained by using (30) and (31) to calculate the total water discharge Q and volumetric sediment discharge Q_s on a given cross-section. After some manipulation the approximate forms

$$\tilde{Q} = 4.97R^{1.70}S^{0.50}B^*(1 - 2.23/\mathcal{A}), \tag{34}$$

$$Q^* = 1.02 \times 10^{-5}R^{0.275}B^*(1 - 4.52/\mathcal{A}) \tag{35}$$

are obtained. Here $\tilde{Q} = Q/[(\mathcal{R}gD_s)^{1/2} D_s^2]$, $Q^* = Q_s/[(\mathcal{R}gD_s)^{1/2} D_s^2]$ and $B^* = B/D_s$; the relations hold for the previously quoted restraints on R and \mathcal{A} . It should be noted

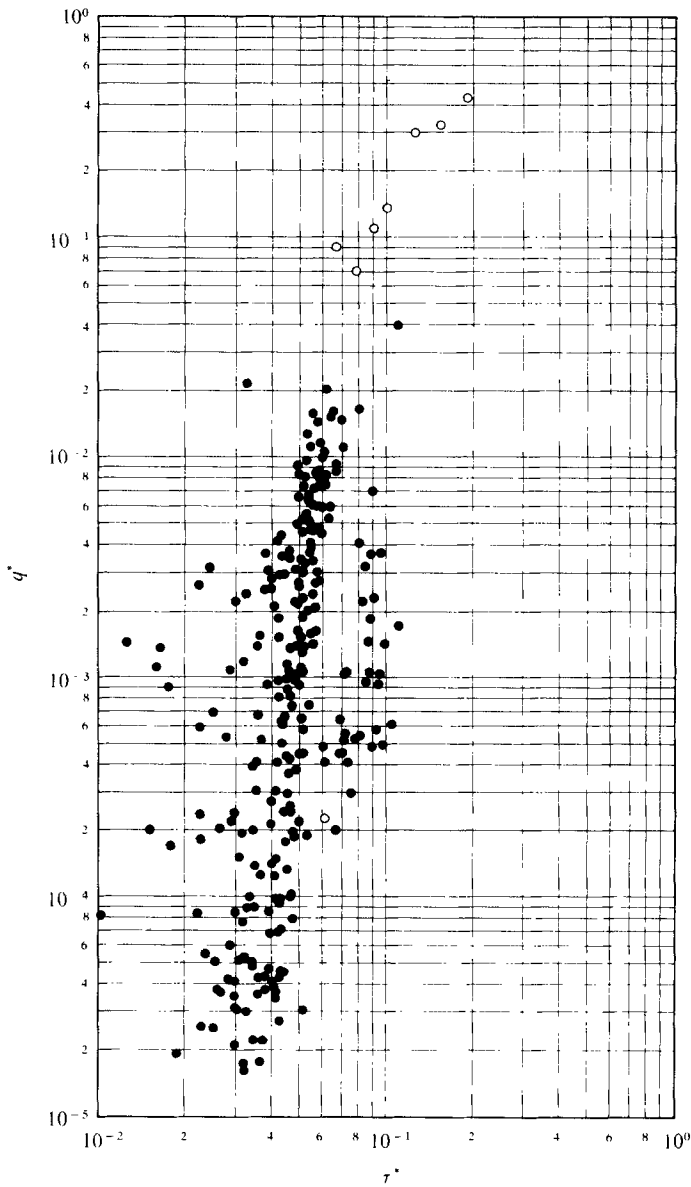


FIGURE 7. Bed load relation for gravel beds.

that (35) is highly sensitive to both inaccuracies in the closure hypothesis and the choice of a load relation, and thus is subject to more inaccuracy than the other two relations.

In summary, the analysis allows for bankfull or dominant bed stress which exceeds the critical stress by about 20%, resulting in a low but non-vanishing rate of sediment transport. Qualitatively this corresponds well to the observations in § 2.

Implicit in the three regime relations is a relation for the bankfull width. If D_{50} and any two of the parameters D_c , B , S , Q and Q_s [except the pair D_c and S , which is constrained by (33)] are known, the other three can be calculated.

9. Limitations of the analysis

Natural rivers are extremely complicated phenomena and it would be facile to assume that the present analysis provides a complete and accurate picture of gravel rivers. To repeat, the regime relations (33)–(35) apply only to straight reaches with bed and banks composed of similar non-cohesive coarse gravel at bankfull or dominant discharge. Reaches approximately satisfying these conditions can be found in nature. However, it is much more typical to find complicating factors present. Among these, alignment variation and the presence of noticeable quantities of sand and fines, particularly in the banks, are important.

Alignment variation includes the phenomena of meandering and braiding. It has been established through stability analysis that straight channels are usually subject to instability leading to a meandering or braiding pattern (e.g. Callander 1969; Engelund & Skovgaard 1973; Parker 1976). The pattern, once established, implies a gradually shifting alignment, the gross characteristics of which are fairly stable when averaged over several bars in the downstream direction.

The River Rheidol, Wales, illustrated in figure 8, provides an example of a river in coarse gravel which maintains a meandering pattern (Lewin 1972). Coarse gravel predominates in the bed and banks up to 30 cm of the top of the flood plain, which is covered with a thin layer of sand and organic material. Fines are nearly absent from the channel and flood plain. Once initiated, meander bends migrate laterally and downstream, increasing their amplitude. This migration is fed by the shear stress distribution and secondary currents generated by the bend itself, which imply erosion at the concave bank and deposition at the convex bank. When the meander amplitude reaches a certain limit, the bend is cut off during a flood and the process is re-initiated (figure 8).

It is clear that alignment variation cannot be the process that maintains the river width. It may be surmised, however, that the process of bar formation, superimposed over the mechanism described herein for maintaining the width of straight channels, might allow channels to migrate while maintaining coherent widths not greatly different from what would be found in a straight stream of the same channel slope. Thus the regime relations presented herein might be expected to provide crude estimates of reach-averaged channel properties of meandering or braiding streams at bankfull discharge.

The presence of noticeable quantities of sand and fines that are transported in suspension at high discharges can lead to the maintenance of substantially narrower, deeper channels, as discussed in the companion paper. This material falls out of suspension and concentrates wherever turbulence is weak, e.g. on the banks and flood plain. If it is available in sufficiently large quantities the level of the flood plain may be raised well above the highest horizon on which gravel lies, and the banks may be covered with this finer material. The mechanism for the maintenance of banks becomes a balance between deposition of material from suspension and erosion rather than the critical-stress condition used herein.

Even if such material does not predominate on the banks, its presence may allow steeper banks and deeper, narrower channels by effectively increasing the angle of repose of the bank gravel. In particular, if bank gravel is imbricated in a matrix containing cohesive material (clay) and allowed to dry during low flow, it becomes

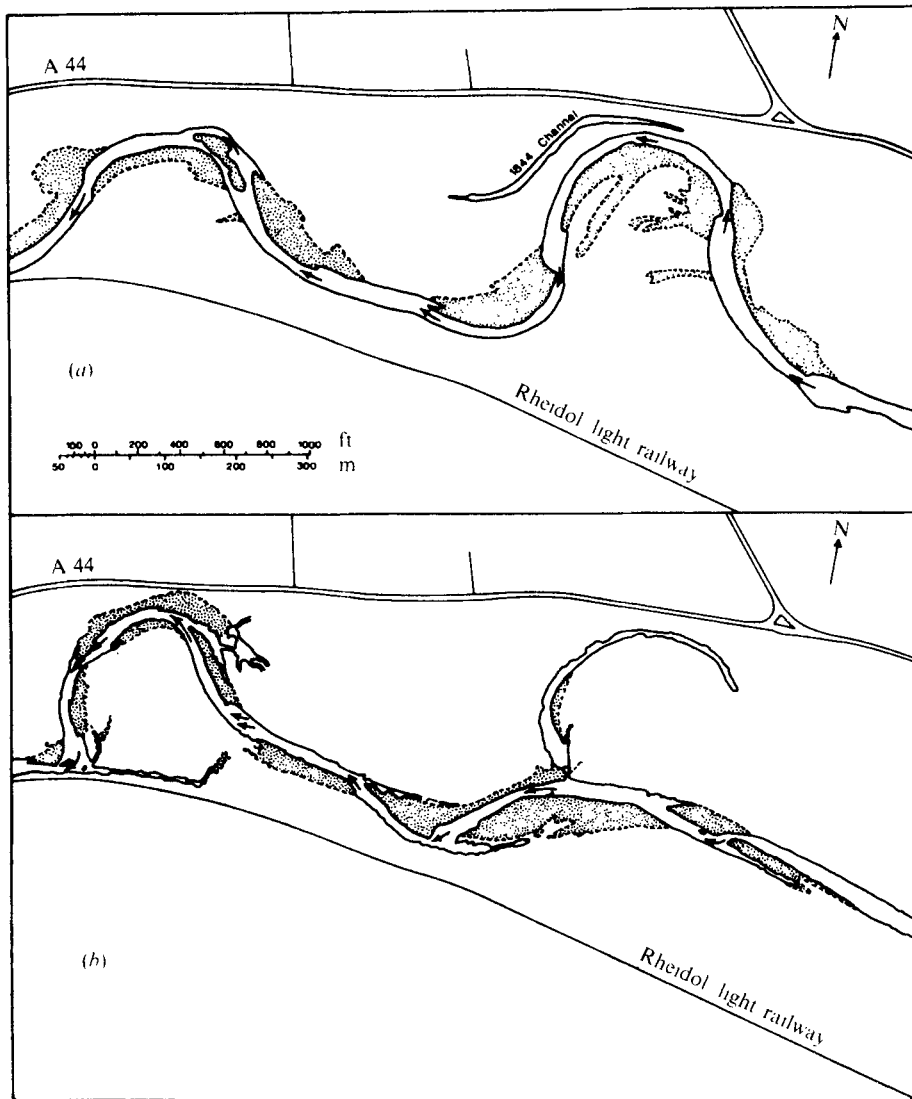


FIGURE 8. Successive planforms of a reach of the Rheidol River, Wales, a meandering gravel stream. (a) Course in 1951. (b) Course in 1971. From Lewin (1972).

cemented in place. Under such circumstances, the banks are less susceptible to erosion during moderate floods. When this effect is present, it is evidenced by steep-cut banks on the outside of bends.

It is also important to note that many rivers with paved gravel beds at lower discharges may contain considerable quantities of material in the sand range available for transport as bed load, as Emmett (1976) has noted. In some cases, this finer load is dominant even though gravel sizes dominate in the bed and banks. It cannot be predicted from (31) or (35).

Other complications are bank vegetation and erosional controls such as bedrock outcrops and valley walls.

River	Source	Q (m ³ /s)	S	B (m)	D_c (m)	D_{50} (mm)	D_{90} (mm)
Athabasca	Neill (1973)	2690	0.00087	206	3.81	45	75
Athabasca	Neill (1973)	2690	0.00081	244	3.81	45	75
Athabasca	Neill (1973)	2690	0.00053	223	5.52	45	75
Chilko	Kellerhals (1963)	159	0.00503	45.7	1.68	142	254
Cariboo	Kellerhals (1963)	340	0.00491	57.9	2.59	267	470
Quesnel	Kellerhals (1963)	419	0.00633	61.0	2.44	216	381
Snake	Emmett (1977)	2600	0.001	190	5.1	64	—
Clearwater	Emmett (1977)	1450	0.00032	140	5.2	64	—
Rheidol	Lewin (1977)	Unknown	0.0025	23.6	0.91	37	—

TABLE 1. Basic data for gravel rivers at dominant discharge.

The present analysis is thus seen to apply to a limiting case in which the width is a maximum and the depth is a minimum, corresponding to the absence of any material other than loose gravel.

10. Comparison with data

In order to determine whether a gravel-river reach is within the limitations of applicability of the regime relations derived herein, it is necessary to have a complete description, including information concerning alignment, cross-sectional shape, bed and bank material, bankfull or dominant discharge (and the method used to determine it), evidence of bed motion, etc. Two sources found to contain the requisite information are Kellerhals (1963) and Neill (1973).

Neill (1973) has divided a 100 km length of the Athabasca River into three reaches. His table 3 summarizes average cross-sectional data for the straight portions of each of these reaches. The discussion in § 2 indicates the applicability of the present analysis to these three reaches. The data used herein are summarized in table 1. The value $D_{50} = 45$ mm has been assumed for all three reaches. Since Neill gives the average depth \bar{D} rather than D_c , D_c has been calculated from the cross-sectional profile derived herein, which implies

$$\bar{D}/D_c = 1 - 1.54D_c/B. \quad (36)$$

The three reaches from Kellerhals (1963) listed in § 2 also satisfy the criteria of evidence of bed mobility, bed and banks composed of coarse gravel, and only moderate deviation from straight alignment, and have been included in table 1. For these reaches D_c was measured directly rather than calculated from \bar{D} . It should be noted that neither investigator has directly measured bed load in these reaches.

Another useful set of data can be found at a vastly differing scale. Wolman & Brush (1961) conducted 16 experiments in coarse sand ($D_{50} = 0.67$ mm) in which self-formed straight stable channels with vanishing suspended load and non-zero bed load were observed. These channels provide nearly exact models of gravel rivers in the sense of similitude. The only source of discrepancy is that $u_{*c} D_{90}/\nu$ is about 20, so the flow is not completely rough. Nevertheless, the discrepancy thus inherent in the use of (12) can be expected to be small.

Expecting that the first two regime relations should provide reasonable estimates for channels with varying alignment, more data were selected from the compilation

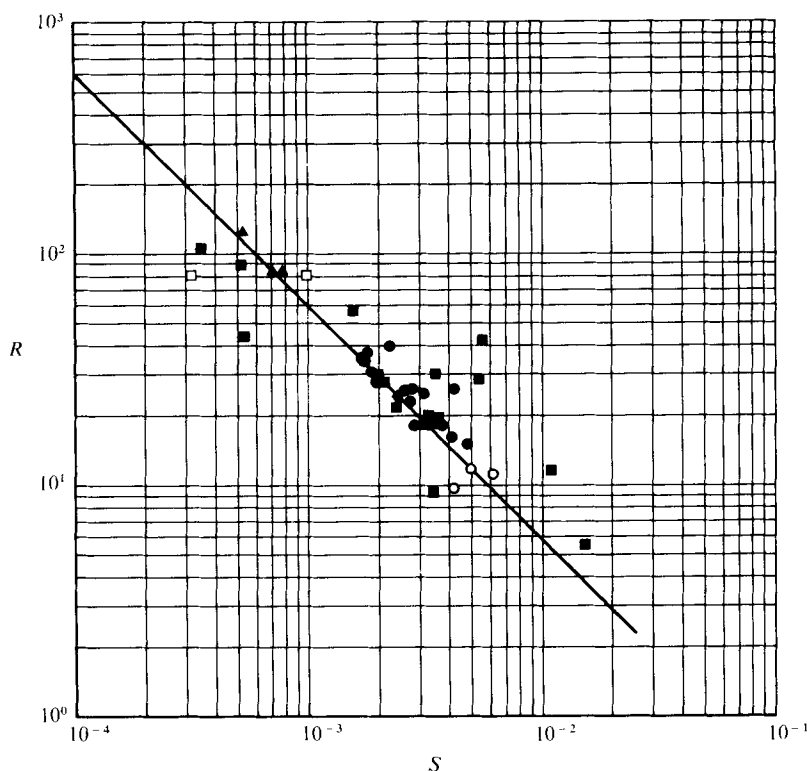


FIGURE 9. Test of the first regime relation (33) (solid line). ■, Kellerhals *et al.* (1972); ○, Kellerhals (1963); ▲, Neill (1973); □, Emmett (1977); ◆, Lewin (1977); ●, Wolman & Brush (1961).

of basic data on rivers in Alberta, Canada, due to Kellerhals *et al.* (1972). Of the reaches for which bankfull conditions are listed, forty-two have beds in which coarse gravel dominates. This list was narrowed to sixteen reaches, the others being eliminated for one or more of the following reasons: (a) a major engineering work such as a dam, weir, canal intake, etc. existed in or near the reach (bridges were excepted); (b) gravel was not a major component of the bank material; (c) bedrock outcrops were present, or erodibility was limited; or (d) the bankfull discharge return period exceeded 25 years. Thus the sixteen reaches selected loosely fulfil the conditions postulated for the analysis herein, except that alignment variation manifested in the form of bar formation associated with meandering and braiding is present. Field rather than map slopes were used where possible (see original reference).

Data for the Clearwater and Snake Rivers, Idaho, were provided by Emmett (1977, private communication) and data for River Rheidol, Wales, were provided by Lewin (1977, private communication). The values are for bankfull conditions and are listed in table 1. The banks of the Rheidol are essentially gravel; those of the Clearwater and Snake are predominantly sand but contain gravel as well.

The total data set comprises 41 reaches, with discharges ranging from 3.1×10^{-4} cumecs to 5.4×10^3 cumecs and centre depths ranging from 1×10^{-2} m to 7.2 m. The first regime relation, (33), is tested directly in figure 9. The second regime relation, (34), can be cast in the form

$$R = 0.866(\tilde{Q}/B^*)^{0.830} \quad (37)$$

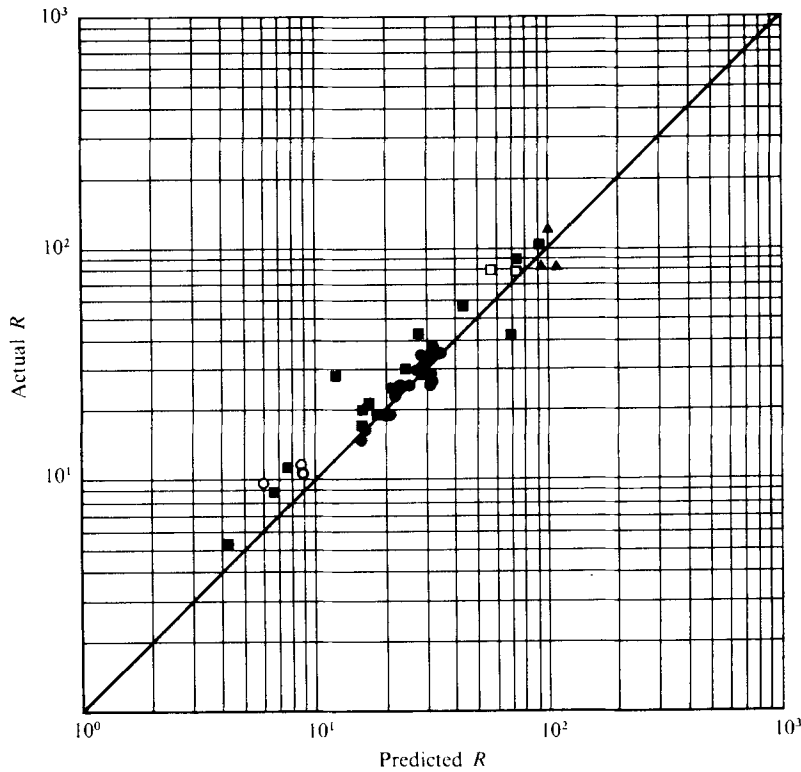


FIGURE 10. Test of the second regime relation (34). Calculated values of R are compared with observed values. Symbols as in figure 9.

for appropriately large aspect ratios. It is tested by using the observed values of \bar{Q} and B^* to calculate R from (37) and then comparing this with the observed value of R , as is done in figure 10. While considerable scatter is present, rough confirmation of (33) and (34) is obtained. It is of interest to note that the laboratory data, although of a scale that differs vastly from that of the field data, fit in among the latter in the dimensionless plots.

The load relation (35) has not been tested owing to its illustrative nature and to a lack of field data.

These regime relations can be used to derive dimensionally homogeneous downstream relations for the hydraulic geometry of gravel streams (Parker 1978).

11. Conclusion

The concept of lateral transfer of downstream momentum by turbulent diffusion embodied in the work of Lundgren & Jonsson (1964) has been used together with singular perturbation techniques to explain the coexistence of stable banks and mobile beds in straight reaches of coarse gravel rivers. The analysis has been used to obtain rational regime relations for such reaches.

Points which deserve further attention are the use of more accurate closure assumptions, a treatment of secondary currents in straight channels, and the inclusion of sediment gradation effects.

Financial support was provided by the United States Agricultural Research Service, the United States National Science Foundation and the National Research Council of Canada. Special thanks are due to Thomas Lundgren, who unknowingly inspired this work, and to N. Rajaratnam, the discussions with whom helped bring it out of limbo.

REFERENCES

- BRUSH, L. M. 1961 Drainage basins, channels, and flow characteristics of selected streams in central Pennsylvania. *U.S. Geol. Survey Prof. Paper* no. 282-F.
- CALLANDER, R. A. 1969 Instability and river channels. *J. Fluid Mech.* **36**, 465–480.
- CRUFF, R. W. 1965 Cross-channel transfer of linear momentum in smooth rectangular channels. *U.S. Geol. Survey Water Supply Paper* no. 1592-B.
- EMMETT, W. W. 1976 Bedload transport in two large, gravel-bed rivers, Idaho and Washington. *Proc. 3rd Federal Inter-Agency Conf., Denver, Colorado.*
- ENGELUND, F. & SKOVGAARD, O. 1973 On the origin of meandering and braiding in alluvial streams. *J. Fluid Mech.* **57**, 289–302.
- GLOVER, R. E. & FLOREY, Q. L. 1951 Stable channel profiles. *U.S. Bur. Reclamation, Hydr.* no. 325.
- HIRANO, M. 1973 River-bed variation with bank erosion. *Proc. Japan Soc. Civil Engrs* no. 210, pp. 13–20.
- HOLLINGSHEAD, A. B. 1971 Sediment transport measurements in gravel rivers. *Proc. A.S.C.E., J. Hydraul. Div.* **97** (HY11), 1817–1834.
- KELLERHALS, R. 1963 Gravel rivers with low sediment charge. M.Sc. thesis, University of Alberta.
- KELLERHALS, R. 1967 Stable channels with gravel-paved beds. *Proc. A.S.C.E., J. Waterways Harbors Div.* **93** (WW1), 63–84.
- KELLERHALS, R., NEILL, C. R. & BRAY, D. I. 1972 Hydraulic and geomorphic characteristics of rivers in Alberta. *Res. Counc. Alberta River Engng Surface Hydrol Rep.* no. 72-1.
- KEULEGAN, G. H. 1938 Laws of turbulent flow in open channels. *Nat. Bur. Stand. Res. Paper* RP 1151.
- LANE, E. W., LIN, P. N. & LIU, H. K. 1959 The most efficient stable channel for completely clean water in non-cohesive material. *Colorado State Univ. Rep.* CER 59 HKL 5.
- LEIGHLY, J. B. 1932 Toward a theory of the morphologic significance of turbulence in the flow of water in streams. *Univ. Calif. Publ. Geogr.* **6**.
- LEWIN, J. 1972 Late-stage meander growth. *Nature Phys. Sci.* **240**, 116–117.
- LI, R. M., SIMONS, D. B. & STEVENS, M. A. 1976 Morphology of cobble streams in small watersheds. *Proc. A.S.C.E., J. Hydraul. Div.* **102** (HY8), 1101–1117.
- LUNDGREN, H. & JONSSON, I. G. 1964 Shear and velocity distribution in shallow channels. *Proc. A.S.C.E., J. Hydraul. Div.* **90** (HY1), 1–21.
- NEILL, C. R. 1968 A re-examination of the beginning of movement for coarse granular bed material. *Hydraul. Res. Station, Wallingford, Berks., Rep.* INT 68.
- NEILL, C. R. 1973 Hydraulic and morphologic characteristics of Athabasca River near Fort Assiniboine. *Res. Counc. Alberta Highway River Engng Div. Rep.* no. REH/73/3.
- PARKER, G. 1976 On the cause and characteristic scales of meandering and braiding in rivers. *J. Fluid Mech.* **76**, 457–480.
- PARKER, G. 1978 Hydraulic geometry of active gravel rivers. *Univ. Alberta Hydrotech. Engng. Rep.*
- PARKER, G. 1978 Self-formed rivers with stable banks and mobile bed. Part 1. The sand-silt river. *J. Fluid Mech.* **89**, 109–125.
- PETERSON, A. W. & HOWELLS, F. R. 1973 A compendium of solids transport data for mobile boundary channels. *Dept. Civil Engng, Univ. Alberta, Rep.* HY-1973-ST3.
- WOLMAN, M. G. & BRUSH, L. M. 1961 Factors controlling the size and shape of stream channels in coarse non-cohesive sands. *U.S. Geol. Survey Prof. Paper* no. 282-G.